



Carbon Supported Platinum-Molybdenum Alloy Nanoparticles for Oxygen Reduction Reaction

NATARAJAN MANIVANNAN^{1,2}, VIJAI SHANKAR BALACHANDRAN² and V.S. VASANTHA^{1,*}

¹Department of Natural Products Chemistry, School of Chemistry, Madurai Kamaraj University, Madurai-625021, India

²Reliance Industries Limited, Reliance Corporate Park, Ghansoli, Navi Mumbai-400701, India

*Corresponding author: E-mail: vasantham999@yahoo.co.in

Received: 10 February 2021;

Accepted: 25 March 2021;

Published online: 16 April 2021;

AJC-20338

Fuel cells are gaining importance in the emerging area of power generation. However, sluggishness of the cathodic oxygen reduction reaction (ORR) and usage of expensive electrocatalysts are hindering its widespread application. Hence, an effort has been made in the present study to synthesize efficient electrocatalysts based on Pt-Mo alloys with varying atomic ratios (0-100 at. %) by thermal decomposition method. The synthesized samples were characterized using XRD, STEM, EDX and XPS techniques. The electrocatalytic activity for ORR was measured using cyclic voltammetry and rotating disk electrode for all the samples and Pt-Mo (1:1) electrocatalyst performed better among the synthesized electrocatalysts with ORR current density of 63 mA/cm² at an applied potential of 0.6 V vs. Hg/HgSO₄. The present study suggests that Pt-Mo studied are proven to be a superior catalyst than a costly Pt catalyst with high ORR activity.

Keywords: Oxygen reduction reaction, Hydrogen oxidation reaction, Lattice constant, Platinum, Molybdenum.

INTRODUCTION

Fuel cell is an energy device producing electrical energy from the chemical energy supplied externally. Platinum catalyst used in fuel cells are expensive and have limited availability. Alloying Pt with other metals like Co, Ru, Sn, Mo, Cu, Fe, Y and Zn showed an enhanced oxygen reduction reaction (ORR) at the cathode and also reduces the usage of platinum at the electrode side [1-3]. Bifunctional catalysts are required for the improved oxygen reduction reaction (ORR) and oxygen evolution reaction (OER) to develop high performance fuel cell. Electronic and geometrical properties of platinum will be modified by alloying with other transition metals and it influences the kinetics of ORR [4-7]. Hydrogen oxidation reaction (HOR) in Pt-Mo alloy is widely studied whereas limited studies are reported on ORR in the same catalyst. As platinum is rich in *d*-electrons compared with molybdenum, alloying of platinum with molybdenum enables the transfer of *d*-electrons from Pt to Mo. As a result of this, the creation of vacancies in platinum 5*d*-band facilitates the reduction of oxygen. Since platinum has a greater number of electrons in the *d*-orbitals, there is a possibility of transfer of these electrons to the *d*-orbital of molybdenum and it creates additional vacancies in the 5*d*-band of

platinum. This effect enhances the adsorption of oxygen on the Pt-Mo surface and helps in easy reduction of oxygen molecule by reducing the binding energy of O-O bond [8,9]. Increasing the amount of molybdenum beyond the certain value (Pt-Mo/C = 3:1) reduce the ORR activity due to the decrease in the number of oxygen adsorption sites on the catalyst surface [4]. The synergistic efficiency of bimetallic nanoparticles demonstrated higher effectiveness than the single metal nanoparticles [10-12]. Kinoshita [8] reported the effect of particle size and distribution of particles on certain crystal faces on ORR activity. Sharma *et al.* [13] reported the synthesis of Pt-Mo/C nanoparticles using impregnation reduction method. They found an increase in the current density with the varying composition of Pt-Mo catalyst in the following order Pt₅₀Mo₅₀ > Pt₇₀Mo₃₀ > Pt₁₀₀Mo₀ > Pt₀Mo₁₀₀.

In the present study, carbon supported Pt-Mo nanoalloy electrocatalysts have been synthesized by simultaneous thermal decomposition of platinum acetylacetonate and molybdenum carbonyl in a solution containing oleyl amine, oleic acid and 1,2-hexadecanediol in the presence of Vulcan XC-72R carbon, followed by annealing at 400 °C in H₂/Ar atmosphere.

This is a modified procedure reported for the preparation of Pd-Mo and Pd-W by simultaneous thermal decomposition

of palladium acetylacetonate and molybdenum/tungsten carbonyl using *o*-xylene [10]. In this study, the structure of Pt-Mo (1:1) catalyst was characterized by X-ray diffraction (XRD), transmission electron microscopy (TEM), X-ray photoelectron spectroscopy (XPS) and the results were compared with Pt/C. Electrochemical behavior was evaluated by cyclic voltammetry and rotating disc electrode (RDE) method. It was concluded that Pt-Mo (1:1)/C alloy catalysts exhibited better O₂ reduction catalytic properties than Pt/C. The total number of electrons transferred during the electrochemical ORR for each of these samples was obtained from Koutecky-Levich plots.

EXPERIMENTAL

Molybdenum hexacarbonyl [(Mo(CO)₆], platinum acetylacetonate [Pt(acac)₂], Vulcan XC-72R, oleyl amine were received from Sigma-Aldrich. Oleic acid and 1,2-hexadecane diol (TCI Chemicals, Japan) were supplied by (TCI Chemicals, Japan). Supra pure grade sulfuric acid was obtained from Merck, Germany. Deionized water (18.2 MΩ.cm; Millipore) was used to prepare all solutions. High-purity Ar and O₂ (grade 5.0) gases were obtained from Mars gas (Mumbai, India) and INOX India (Vadodara, India), respectively.

Electrocatalysts synthesis: In a typical preparation of Pt-Mo (1:1 at wt. ratio) 30 mg of platinum acetylacetonate, 20 mg of molybdenum hexacarbonyl, and 80 mg of Vulcan XC-72R were taken in a 5-necked flask and mixed well under Ar atmosphere [14]. Then the solution containing 10 mL of oleyl amine, 4 mL of oleic acid and 15 mg of 1,2-hexadecanediol was added to the reaction mixture in dropwise manner. After the addition, the reaction mixture was refluxed for 6 h under Ar atmosphere. After 6 h, the solvent and unreacted diol were extracted with the mixture containing ethanol and hexane (20:80% v/v), and then the residue was transferred to a petri dish. Finally, the residue was heated at 400 °C for 4 h in a furnace under H₂/Ar (1:5) atmosphere and henceforth, these powder samples are referred as electrocatalysts and the final mass loading of the Pt and Mo metals were in the molar ratio of 1:1. Similarly, by varying the proportion of platinum acetylacetonate and molybdenum hexacarbonyl, Pt-Mo (2:1 at. wt. ratio) and Pt-Mo (3:1 at. wt. ratio) were prepared. Carbon-supported Pt catalyst with 20 wt.% metal in carbon was also synthesized by refluxing required amounts of platinum acetylacetonate with hexadecanediol as a reducing agent and Vulcan XC-72R carbon black in oleic acid and oleyl amine. The expected quantity and the yield of the catalyst are presented in Table-1.

Based on the preliminary electrochemical studies conducted using cyclic voltammetry, further studies on the characterization and evaluation of the catalysts was confined to Pt-Mo (1:1)/C that yielded the maximum electrochemical surface area.

Characterization techniques: The Powder X-ray diffraction (XRD) spectra were recorded on D8 Discover (Bruker GmbH) in bragg-brentano geometry. The XRD spectra were recorded in the scan range of $2\theta = 10-80^\circ$. The phase formation was obtained using X'pert High score Plus (version 2.1.0) software by referring the international Centre for Diffraction Data. The XPS analysis was carried out on K-alpha (ThermoFisher, USA). TEM and EDX were done in TITAN G2 60-300 (ThermoFisher USA). The samples were dispersed on holey carbon supported on copper grids (200 mesh) from a hexane dispersion (Electron Microscopy Sciences, USA). HAADF-STEM images were acquired at 300keV. The EDX elemental mapping was done with at least 1000 kcps using Espirit 1.9 software. Each imaging was done for minimum 30 min for proper elemental mapping [15].

Preparation of the working electrode: A 20 wt. % of Pt-Mo (1:1) was dispersed on carbon (2 mg) in the solution containing deionized water (2 mL) and 5 wt.% of Nafion solution (20 μL, Sigma-Aldrich) in order to prepare catalyst ink. The resulting mixture was under ultrasonication for 15 min to obtain a homogeneous black ink. Catalyst ink was drop-casted on polished glassy carbon electrode (5 mm diameter) and dried using infrared lamp for 15 min. Prior to drop-casting, the surface of the electrode was polished with 50 nm alumina [16].

Electrochemical measurements: Electrochemical measurements with three-electrode cell arrangement was carried out for the prepared electrocatalyst samples. The electrocatalyst ink was applied by drop-casting method over the surface of glassy carbon (GC) electrode, which was used as the working electrode. The Hg/HgSO₄ (filled with saturated K₂SO₄ electrolyte) and platinum wire were used as the reference and counter electrodes, respectively. Electrochemical experiments were carried out in O₂ gas (99.999 %, Mars Gas, Mumbai, India) saturated 0.5 M H₂SO₄ solution [17].

Rotating disc voltammetry: Pt-Mo (1:1) oxygen reduction reaction (ORR) activity was quantified using a rotating disk electrode (AFMSRCE, Pine Research Instrumentation, USA). The purified electrocatalyst coated GCE was fixed in the RDE assembly, controlled by MSR rotator (AFMSRCE, Pine Research Instrumentation, USA). Rotating disc electrode (RDE) was immersed in a three-electrode cell having a 0.5 M H₂SO₄ as an electrolyte (500 mL) along with purging and saturation with O₂ gas (99.999%, Mars Gas Company, Mumbai) [2,18].

RESULTS AND DISCUSSION

The recorded diffraction patterns of Pt-Mo (1:1)/C catalyst are shown in Fig. 1. The peak at $2\theta = 24^\circ$ can be referred to the (002) plane of Vulcan XC-72 carbon. The XRD peaks at 40.05° , 46.65° and 68.03° can be ascribed to the (111), (200)

TABLE-1
ATOMIC AND WEIGHT PERCENTAGES OF Pt AND Mo METALS FOR CATALYST PREPARATION

Catalyst/ Alloys	Atomic (%)		Weight (%)		Weight (mg)		Weight of alloy/catalyst (mg)	Weight of alloy/catalyst after heating (mg)
	Mo	Pt	Mo	Pt	Mo	Pt		
Pt	–	100.00	–	100.00	–	20.00	20	–
MoPt	50.00	50.00	32.95	67.05	6.59	13.41	20	18.0
MoPt ₂	33.33	66.67	19.74	80.26	3.95	16.05	20	16.1
Mo ₃ Pt ₂	60.00	40.00	42.45	57.55	8.49	11.51	20	15.2

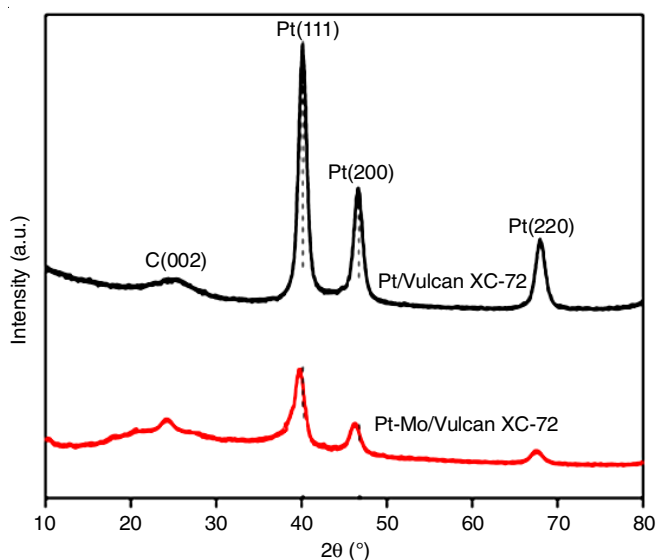


Fig. 1. XRD of Pt/Vulcan XC-72 and Pt-Mo (1:1)/Vulcan XC-72

and (220) planes, respectively, of the FCC planes of platinum. According to JCPDS card no.70-2057, diffraction at 39.8° ,

46.2° and 67.6° referred to Pt (111), Pt (200) and Pt (220) crystal planes, respectively. The shift in the XRD peak observed for platinum in Pt-Mo (1:1)/C catalysts indicate the lattice contraction effect due to the alloying effect. This shift is low in the case of platinum in Pt/C. This is corroborated from the lattice parameter value for (111) plane of platinum nanoparticles in Pt-Mo (1:1) alloy calculated using the Bragg equation, which is 0.3893 nm less than the value 0.3920 nm for platinum in Pt/C. The average particle size of the Pt-Mo (1:1)/Vulcan XC-72 catalyst was measured using the Scherrer formula [19] and was calculated as ~ 7.3 nm [20,21].

XPS analysis: The various composition and different chemical oxidation states at the catalyst surface, which contains Pt, Mo, C and O in the Pt-Mo (1:1)/Vulcan XC-72 were examined by XPS analysis. The survey scans of the Pt-Mo (1:1)/Vulcan XC-72 is shown in Fig. 2a, which clearly indicates the presence of Pt, Mo, C, and O elements on the surface of sample. Fig. 2b shows the deconvolution of Mo 3d-peak in to doublets. Strong peaks observed at 229.6 and 232.5 eV are ascribed to the binding energies of Mo $3d_{5/2}$ and Mo $3d_{3/2}$ of Mo^{4+} . The peak raised at 234.1 eV is the binding energy of Mo $3d_{3/2}$ and

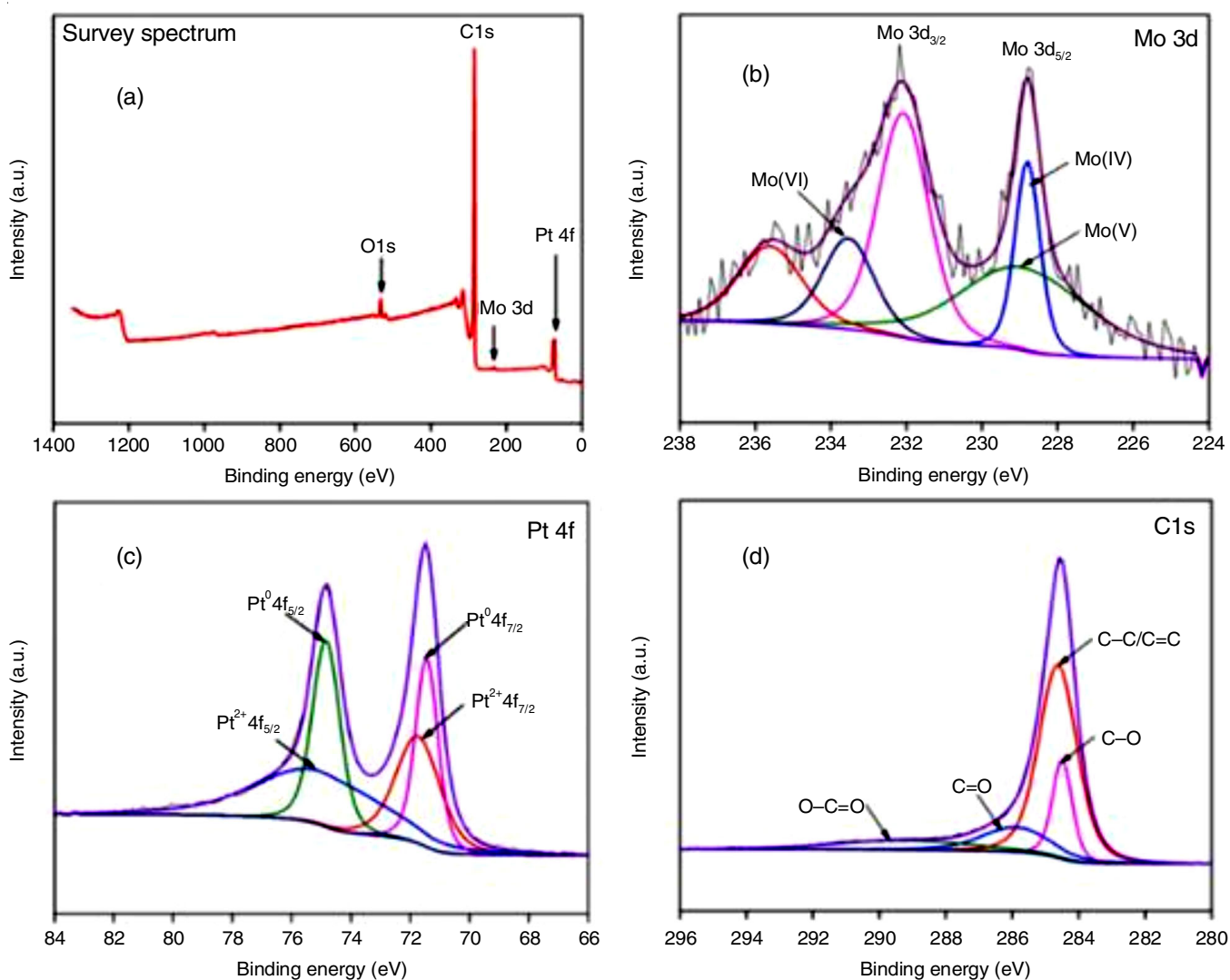


Fig. 2. XPS spectra of Pt-Mo (1:1)/Vulcan XC-72. (a) The survey spectrum, (b) Mo 3d, (c) Pt 4f, and (d) C 1s

indicates the Mo(IV) oxidation state in MoO₂. The spectral peaks at 230.6 and 235.5 eV ascribed to states of Mo(VI) 3d_{5/2} and 3d_{3/2} of MoO₃, respectively, depicts the slight surface oxidation of metastable MoO₂ in air. The most predominant peaks of Pt⁰ state is referred by the deconvoluted-doublets peaks of Pt 4f spectrum of Pt-Mo (1:1)/Vulcan XC-72 as shown in Fig. 2c. The two prominent peaks of 72.37 and 76.12 eV shows Pt 4f spectra may be ascribed to the platinum in oxide form (Pt²⁺ state) such as PtO and Pt(OH)₂ due to the surface oxidation. The C1s spectrum (Fig. 2d) of Pt-Mo (1:1) Vulcan XC-72 shows the presence C=C, C-O-C, C-O and O-C=O functional groups [22]. The ratio of Pt:Mo measured using the XPS was 1:0.7, which suggests that the surface of synthesized electrocatalyst was enriched with platinum metal [14,23].

TEM analysis: The morphology of the synthesized Pt-Mo (1:1)/Vulcan XC-72 electrocatalyst was analyzed using HR-TEM images. Fig. 3a shows that the Pt-Mo (1:1) nanoparticles dispersed on Vulcan XC-72 and shows the presence of bright dots. It is reported that the presence of noble metals displays bright dots in the HAADF-STEM [24,25], hence these dots may confirm the presence of Pt and Mo metals in the synthesized samples. Further, gray contrast generated may be due to the presence of carbon [14].

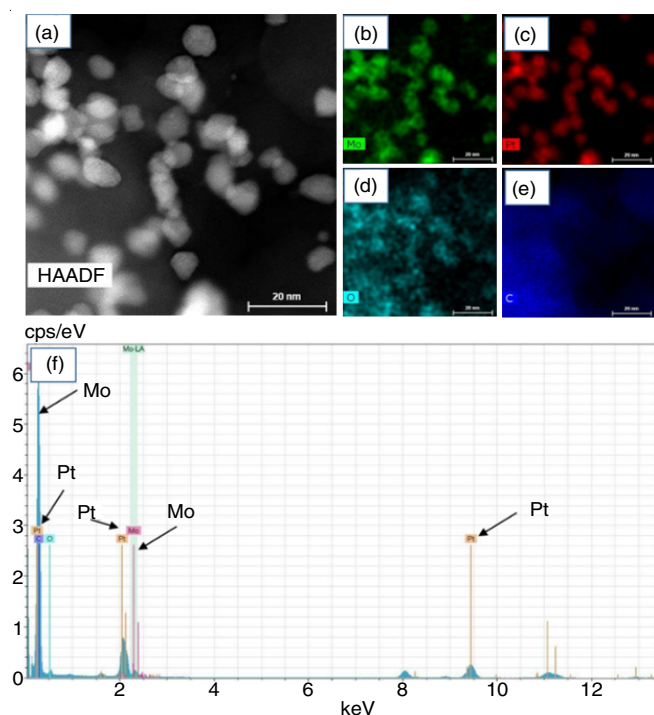


Fig. 3. (a) HR-TEM images of Pt-Mo (1:1)/Vulcan XC-72. Elemental mapping of (b) Mo, (c) Pt, (d) O and (e) C. (f) EDX analysis of Pt-Mo (1:1)/Vulcan XC-72 showing the presence of Mo and Pt

The particle size was observed in the range of 1 to 10 nm. The dispersion of metallic nanoparticles on the carbon support was observed. The SEM-EDX elemental mapping was carried for individual elements (Pt, Mo, C and O) which were present in the Pt-Mo (1:1)/Vulcan XC-72 sample and are shown in Figs. 3b-e. Fig. 3f shows the STEM-EDX mapping of Pt-Mo (1:1)/Vulcan XC-72R [20].

Electrochemical surface area (ECSA) analysis: The effective catalytic site plays a major role in determining the electrochemical activity is studied by the electrochemical surface area (ECSA) analysis. The ECSA analysis of Pt-Mo (1:1)/Vulcan XC-72 and Pt/Vulcan XC-72 were estimated using cyclic voltammetry (CV) in Ar saturated 0.5 M solution of H₂SO₄ done at 50 mV s⁻¹ (Fig. 4). The ECSA value was obtained according to the following formula:

$$\text{ECSA} = \frac{Q_H}{[\text{Pt}] \times 0.21} \quad (1)$$

where Q_H is the Columbic charge obtained by the area subtended by hydrogen adsorption peaks (between -0.6 and -0.4 V vs. Hg/HgSO₄); [Pt] refers to the total platinum loading (g cm⁻²) of the electrode. The calculated results showed that Pt-Mo (1:1)/C exhibits a ~3x higher ECSA value (94 m² g⁻¹) than Pt/C (33 m² g⁻¹) synthesized using identical method [20].

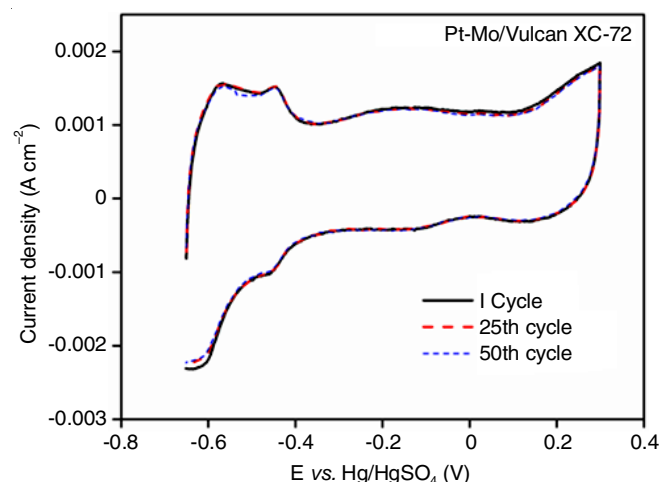


Fig. 4. Cyclic voltammogram of Pt-Mo (1:1)/Vulcan XC-72 at a scan rate of 50 mV s⁻¹

Oxygen reduction reaction (ORR) analysis: The ORR activity was studied in oxygen-saturated 0.5 M H₂SO₄ at 5 mV s⁻¹ with different rotation speeds of 200, 400, 800, 1200 and 1600 rpm. Fig. 5a shows the the polarization curves of Pt-Mo (1:1)/C. The peak current density of value 4.6 mA cm⁻² measured for the oxygen reduction at 1600 rpm. It was found that the oxygen reduction current increases with the rotation speed.

Koutecky-Levich (K-L) equation gives the number of electrons transferred per oxygen molecule during ORR process.

$$\frac{1}{i} = \frac{1}{i_k} + \frac{1}{i_{dl}} \quad (2)$$

where *i* is the current density, *i_k* is the kinetic current density, and *i_{dl}* is the diffusion-limiting current density, given by the following equations:

$$i_{dl} = B\omega^{1/2} \quad (3)$$

$$B = 0.62nF C_{O_2} D_{O_2}^{3/2} \gamma^{-1/6} \quad (4)$$

where B = Levich slope; ω = electrode rotation rate; n = number of electrons transferred in the reduction process; F = Faraday's

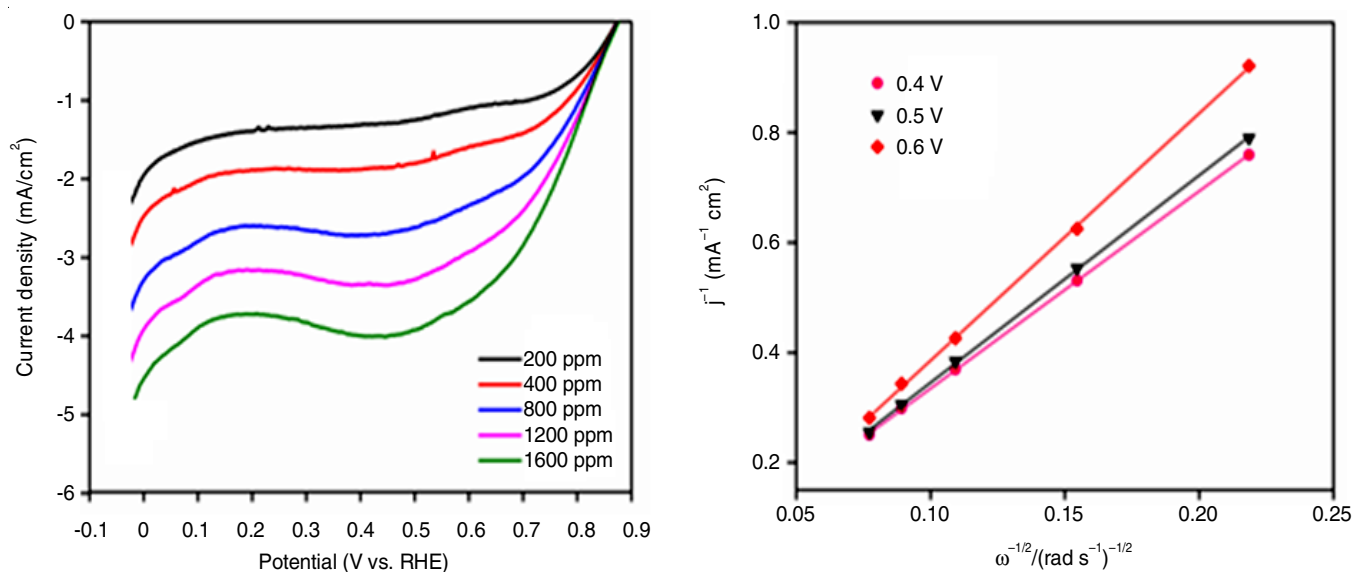


Fig. 5. (a) RDE measurements of Pt-Mo (1:1)/Vulcan XC-72 catalyst in O₂ saturated 0.5M H₂SO₄ at a scan rate of 5 mV s⁻¹ and at different rotation speed (200, 400, 800, 1200 and 1600 rpm); (b) Koutechy-Levich plots (j^{-1} versus $\omega^{-0.5}$) from RDE measurements of Pt-Mo (1:1)/C

constant (96,500 C mol⁻¹); C_{O₂} the concentration of oxygen dissolved in the electrolyte (1.1 × 10⁻⁶ mol cm⁻³); D_{O₂} = diffusion coefficient of dissolved oxygen in 0.5 M H₂SO₄ (1.4 × 10⁻⁵ cm² s⁻¹); and γ = kinematic viscosity of the electrolyte (1 × 10⁻² cm² s⁻¹) [26,27].

The Koutechy-Levich (i^{-1} vs. $\omega^{-1/2}$) plot of Pt-Mo (1:1)/Vulcan XC-72 from ORR data in 0.5 M H₂SO₄ at various electrode potential is shown in Fig. 5b. From the K-L plot, the average number of electrons (n) released per oxygen molecule was found as 4.0, indicating that the reaction mechanism takes place through a four-electron pathway.

Tafel analysis: The polarization curve (Fig. 5a) recorded at 1200 rpm used for measuring the ORR electrocatalytic activity of the synthesized Pt-Mo (1:1) electrocatalyst has been utilized for the Tafel analysis. The data are corrected for diffusion effect using the following expression.

$$j_k = \frac{j_L j}{j_L - j} \quad (5)$$

where, j_k = kinetic current density; j_L = limiting current density, and j = measured current density.

The Tafel slope was obtained by plotting applied potential versus log of current density (j). The Tafel plot in Fig. 6 shows two distinct slopes indicating a break in the Tafel plot due to the change in O₂ reduction mechanism. However, Parthasarathy *et al.* [9] attributed to low Tafel slope to the region where O₂ reduction occurs on a Pt-oxide covered surface while the high Tafel slope is assigned to the region where O₂ reduction occurs on oxide-free Pt surface (-120 mV/decade). The two slopes values calculated from the Tafel plot were 49 mV/dec and 108 mV/dec in agreement with the literature for carbon supported Pt catalysts [28].

Conclusion

The platinum-molybdenum (1:1) alloy nanoparticles supported on the carbon exhibits electrochemical behaviour both

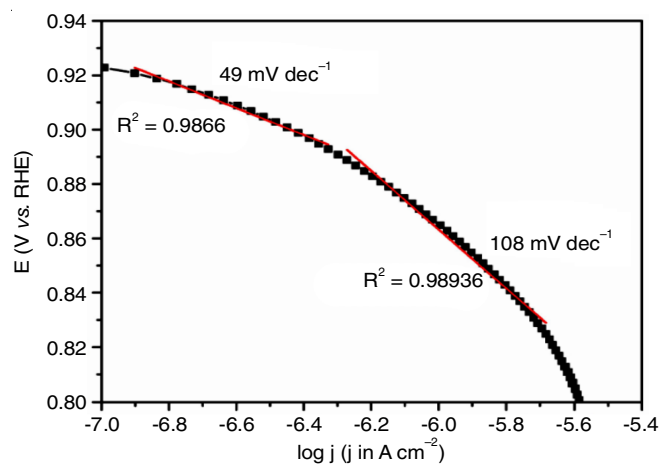


Fig. 6. Tafel slope by plotting applied potential versus log of current density (j)

towards H₂ oxidation and oxygen reduction rate (ORR). Addition of molybdenum lowers the platinum particle size which enhances the electrochemical surface area and thereby improves the ORR. The Pt-Mo (1:1) alloy nanoparticles having particle size less than 7.3 nm was synthesized by facile technique. The Koutechy-Levich analysis revealed that four electrons were involved in the oxygen reduction reaction, which further suggests direct reduction of molecular oxygen to water. The Pt-Mo (1:1) electrocatalyst performed better among the synthesized electrocatalysts with ORR current density of 63 mA/cm² at an applied potential of 0.6 V versus Hg/HgSO₄, while the reported data of Pt-Mo/C (3:1) showed the best performance with a maximum ORR current density of 21.14 mA cm⁻².

ACKNOWLEDGEMENTS

One of the authors (N. Manivannan) is thankful to Prof. Dr. Arindam Sarkar of IIT Bombay, Mumbai, India for providing the lab facilities and guidance.

CONFLICT OF INTEREST

The authors declare that there is no conflict of interests regarding the publication of this article.

REFERENCES

1. T. Reier, M. Oezaslan and P. Strasser, *ACS Catal.*, **2**, 1765 (2012); <https://doi.org/10.1021/cs300309z>
2. C. Wang, M. Chi, D. Li, D. Van Der Vliet, G. Wang, Q. Lin, J.F. Mitchell, K.L. More, N.M. Markovic and V.R. Stamenkovic, *ACS Catal.*, **1**, 1355 (2011); <https://doi.org/10.1021/cs200328z>
3. J.R. McKone, B.F. Sadtler, C.A. Werlang, N.S. Lewis and H.B. Gray, *ACS Catal.*, **3**, 166 (2013); <https://doi.org/10.1021/cs300691m>
4. J. Gao, J. Zou, X. Zeng and W. Ding, *RSC Adv.*, **6**, 83025 (2016); <https://doi.org/10.1039/C6RA16142A>
5. I. Mahesh and A. Sarkar, *ChemElectroChem*, **3**, 836 (2016); <https://doi.org/10.1002/celec.201500452>
6. P.A. Zosimova, A.V. Smirnov, S.N. Nesterenko, V.V. Yuschenko, W. Sinkler, J. Kocal, J. Holmgren and I.I. Ivanova, *J. Phys. Chem. C*, **111**, 14790 (2007); <https://doi.org/10.1021/jp073410j>
7. E.I. Santiago, L.C. Varanda and H.M. Villullas, *J. Phys. Chem. C*, **111**, 3146 (2007); <https://doi.org/10.1021/jp0670081>
8. K. Kinoshita, *J. Electrochem. Soc.*, **137**, 845 (1990); <https://doi.org/10.1149/1.2086566>
9. A. Parthasarathy, S. Srinivasan, A.J. Appleby and C.R. Martin, *J. Electrochem. Soc.*, **139**, 2530 (1992); <https://doi.org/10.1149/1.2221258>
10. A. Sarkar, A.V. Murugan and A. Manthiram, *J. Mater. Chem.*, **19**, 159 (2009); <https://doi.org/10.1039/B812722K>
11. J. Wang and H. Gu, *Molecules*, **20**, 17070 (2015); <https://doi.org/10.3390/molecules200917070>
12. N. Becknell, C. Zheng, C. Chen, Y. Yu and P. Yang, *Surf. Sci.*, **648**, 328 (2016); <https://doi.org/10.1016/j.susc.2015.09.024>
13. A. Sharma, S.K. Mehta, S. Singh and S. Gupta, *J. Appl. Electrochem.*, **46**, 27 (2016); <https://doi.org/10.1007/s10800-015-0900-6>
14. R. Loukrakpam, B.N. Wanjala, J. Yin, B. Fang, J. Luo, M. Shao, L. Protsailo, T. Kawamura, Y. Chen, V. Petkov and C.J. Zhong, *ACS Catal.*, **1**, 562 (2011); <https://doi.org/10.1021/cs200022s>
15. X. Ren, Q. Lv, L. Liu, B. Liu, Y. Wang, A. Liu and G. Wu, *Sustain. Energy Fuels*, **4**, 15 (2020); <https://doi.org/10.1039/C9SE00460B>
16. R. Sankannavar and A. Sarkar, *Int. J. Hydrogen Energy*, **43**, 4682 (2018); <https://doi.org/10.1016/j.ijhydene.2017.08.092>
17. J.A. Gilbert, N.N. Kariuki, R. Subbaraman, A.J. Kropf, M.C. Smith, E.F. Holby, D. Morgan and D.J. Myers, *J. Am. Chem. Soc.*, **134**, 14823 (2012); <https://doi.org/10.1021/ja3038257>
18. A. Ignaszak, C. Song, W. Zhu, Y.J. Wang, J. Zhang, A. Bauer, R. Baker, V. Neburchilov, S. Ye and S. Campbell, *Electrochim. Acta*, **75**, 220 (2012); <https://doi.org/10.1016/j.electacta.2012.04.111>
19. H. Ye, J.A. Crooks and R.M. Crooks, *Langmuir*, **23**, 11901 (2007); <https://doi.org/10.1021/la702297m>
20. R.F.B. De Souza, J.C.M. Silva, M.H.M.T. Assumpção, A.O. Neto and M.C. Santos, *Electrochim. Acta*, **117**, 292 (2014); <https://doi.org/10.1016/j.electacta.2013.11.129>
21. X. Yu and S. Ye, *J. Power Sources*, **172**, 133 (2007); <https://doi.org/10.1016/j.jpowsour.2007.07.049>
22. K.J. Uffalussy, B.K. Captain, R.D. Adams, A.B. Hungria, J.R. Monnier and M.D. Amiridis, *ACS Catal.*, **1**, 1710 (2011); <https://doi.org/10.1021/cs2003559>
23. S. Beyhan, C. Coutanceau, J.M. Léger, T.W. Napporn and F. Kadirgan, *Int. J. Hydrogen Energy*, **38**, 6830 (2013); <https://doi.org/10.1016/j.ijhydene.2013.03.058>
24. G. Chen, Y. Li, D. Wang, L. Zheng, G. You, C.J. Zhong, L. Yang, F. Cai, J. Cai and B.H. Chen, *J. Power Sources*, **196**, 8323 (2011); <https://doi.org/10.1016/j.jpowsour.2011.06.048>
25. M.A. Islam, M.A.K. Bhuiya and M.S. Islam, *Asia Pacific J. Energy Environ.*, **1**, 103 (2014); <https://doi.org/10.18034/apjee.v1i2.215>
26. Z. Xu, C. Shen, Y. Hou, H. Gao and S. Sun, *Chem. Mater.*, **21**, 1778 (2009); <https://doi.org/10.1021/cm802978z>
27. K. Matsutani, K. Hayakawa and T. Tada, *Platin. Metal Rev.*, **54**, 223 (2010); <https://doi.org/10.1595/147106710X523698>
28. U.A. Paulus, T.J. Schmidt, H.A. Gasteiger and R.J. Behm, *J. Electroanal. Chem.*, **495**, 134 (2001); [https://doi.org/10.1016/S0022-0728\(00\)00407-1](https://doi.org/10.1016/S0022-0728(00)00407-1)